Development of Reduced-Intensity Computer Models for Resonant Converters

Arash Fazel Darbandi, Shaahin Filizadeh

Abstract -- **This paper presents a low-intensity average value model for a resonant dc-dc converter using the concept of generalized state-space averaging. This model takes advantage of the periodic nature of the converter operation and represents its response using the time-domain evolution of its Fourier series coefficients. Reduced computational intensity is obtained through neglecting high-frequency switching components. The usefulness of the developed average-value model is demonstrated for a multi-converter resonant system.**

***Keywords*: dc-dc resonant converter, generalized state-space averaging, EMT simulation.**

I. Introduction

MODERN power systems increasingly rely on advanced power electronics to provide controllability and flexibility in the way real and reactive power flow in the network [1-3]. Power electronic converters are also the enabling means of connecting renewable energy sources into the existing grid [4]. Despite their fundamental role in these undertakings, power electronic converters do suffer from limiting factors such as high switching losses and electromagnetic interference (EMI), particularly when high-frequency pulse-width modulation (PWM) techniques are adopted [5-7].

Resonant power-electronic converters offer an alternative and appealing solution in that they allow high-quality conversion with the possibility of significantly reducing the associated switching losses [5-7]. Reduction of losses is achieved through soft-switching techniques such as zero-voltage or zero-current switching. Additionally, by allowing increased switching frequency without incurring additional losses, these converters can operate with smaller and more compact energy storage elements.

Operation at high switching frequencies poses significant challenges in developing computationally efficient models for the electromagnetic transient (EMT) simulation of resonant converters. To capture the operation of the system, excessively small simulation time-steps need to be used, which prolong the simulation time and may also result in numerical inaccuracies. These challenges are only exacerbated when multiple converters are operated in concert, a situation that is frequently encountered in practice. Development of reduced-intensity computer models for resonant converters is, therefore, an important undertaking that eases the design and computer simulation of resonant multi-converter systems.

The paper presents a low-intensity average-value model for resonant dc-dc converters using the concept of generalized state-space averaging [8]. This model takes advantage of the quasi-periodic nature of the converter operation and represents its response using the time-domain evolution of its Fourier series coefficients. The model represents the average dynamic behavior of the converter, and is shown to be adequately detailed for system-level design and controller tuning purposes. The model is capable of representing the average behavior of the converter without having to consider its switching-frequency content. The model also allows inclusion of additional Fourier coefficients, if desired, to increase its accuracy.

The developed average model is verified against a fully-detailed EMT model of the converter. Case studies are presented, in which average-value models for multiple converter systems are developed and compared with the EMT models in terms of accuracy and simulation run-time.

II. Resonant Converter Circuitry and Operation

Figure 1 represents a simplified circuit configuration of a dc-dc resonant converter. It consists of an inverter, a resonant tank and a rectifier. The purpose of the dc-ac inverter is to generate a square wave voltage from a fixed dc voltage source. The generated square-wave waveform has a fundamental frequency sinusoidal component, which can be extracted using a low-pass filter. Therefore, a passive resonant low-pass filter can be designed in such a way to generate an essentially sinusoidal waveform from the given square wave.

The generated sinusoidal waveform can be rectified as shown in Figure 1. The rectified waveform contains a dc component. An adequately large capacitor is usually employed to remove the dc component and to provide energy for the load.

The authors are with the Department of Electrical and Computer Engineering, University of Manitoba, 75 Chancellor Circle, R3T 5V6, Winnipeg, MB, CA (e-mail: umfazeld@cc.umanitoba.ca (corresponding author), shaahin.filizadeh@ad.umanitoba.ca).

Paper submitted to the International Conference on Power Systems Transients (IPST2013) in Vancouver, Canada July 18-20, 2013.

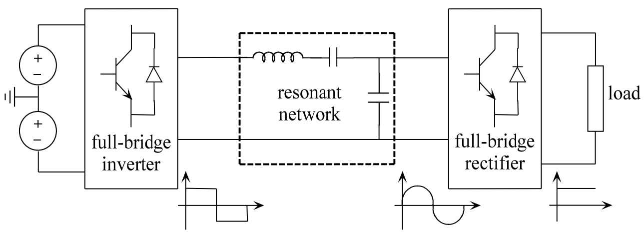

Fig. 1. Simplified circuit diagram of a resonant converter.

III. Generalized State-Space Averaging of Resonant Converters

The characteristic switching operation of power electronic converters leads to periodic changes in the circuit configuration, and hence a non-linear dynamical system [8-10]. For each combination of the states of the switching devices, a separate set of equations is to be defined to describe the circuit. Successive solution of these equations while maintaining continuity of state variables (e.g. capacitor voltages and inductor currents), yields the complete solution of the circuit. Given that each switching state typically only lasts for a short period of time and is followed by another state, the number of sets of equations describing the dynamics of the circuit becomes large and its solution requires massive and time-consuming calculations [9-12].

In generalized state-space averaging technique [8], quasi-periodic circuit variables are described using their time-varying Fourier components. State equations are developed for each Fourier component to determine its evolution with time. It is often observed that a small number of Fourier components are adequate to describe the time-domain variation of the variables of interest with reasonable accuracy. This implies that low-order average-value models can be obtained by only considering one or a few components of the Fourier representation. Addition of more components increases the accuracy at the expense of computational intensity.

A. Mathematical Background of Generalized State-Space Averaging

The method is developed based on the assumption that waveform $x(t)$ can be approximated on the interval $(t - T, t]$ with Fourier series representation of the following form.

$$x(t-T+s) = \sum_{k=-\infty}^{+\infty} \langle x \rangle_k (t) e^{jk\omega_s (t-T+s)} \tag{1}$$

where $\omega_s = \frac{2\pi}{T}$, $s \in (0, T]$, and $\langle x \rangle_k (t)$ are the complex Fourier coefficients [8]. The complex Fourier coefficients are determined as shown in (2).

$$\langle x \rangle_k (t) = \frac{1}{T} \int_{t-T}^{t} x(s) \cdot e^{-jk\omega_s s} ds \tag{2}$$

This expression denotes the Fourier coefficients of the function calculated over a single period of the periodic function, i.e. $(t - T, t]$.

Certain properties of Fourier coefficient such as differentiation with respect to time (3) and convolution (4) are necessary to analyze and convert state equations into complex form [8].

$$\frac{d}{dt} \langle x \rangle_k (t) = \left\langle \frac{d}{dt} x \right\rangle_k (t) - jk\omega_s \langle x \rangle_k (t) \tag{3}$$

$$\langle x \cdot y \rangle_k = \sum_i \langle x \rangle_{k-i} \cdot \langle y \rangle_i \tag{4}$$

Index $k = 0$ indicates the dc component of a given waveform, and index $k = 1$ specifies the fundamental component.

B. Average-Value Model of the DC-DC Resonant Converter

A dc-dc resonant converter with a high-frequency isolating transformer is shown in Figure 2. The schematic diagram also shows additional elements for representation of the load and the source. A resistance (R_r) in series with the resonant tank represents the resistive losses of the tank.

The circuit presented in Figure 1 is used as a reference to develop the underlying equations that describe the dynamics of the resonant converter. The output voltage of the inverter is a square wave with a frequency equal to the switching frequency. Therefore, the voltage waveform at the inverter output can be shown mathematically as follows.

$$v_s = V_{dc} \cdot sign(\sin \omega_s t) \tag{5}$$

where V_{dc} is the magnitude of input voltage source and $sign(x)$ is the sign function defined in (6).

$$sign(x) = \begin{cases} 1 & x > 0 \\ 0 & x = 0 \\ -1 & x < 0 \end{cases} \tag{6}$$

The input voltage to the rectifier is in phase with the resonant tank inductor current to ensure the switching occurs at zero crossing and can be shown as follows.

$$v_R = n \cdot v_s \cdot sign(i_s) \tag{7}$$

where n is the transformer turns ratio. Similarly, the rectifier output current can be mathematically shown as follows.

$$I = abs(i_R) \tag{8}$$

Equations (9) to (12) summarize the mathematical representation of the entire resonant converter.

$$\frac{di_s}{dt} = \frac{1}{L_r}\left(v_s - R_r i_s - v_{Cr} - \frac{1}{n} v_R \right) \tag{9}$$

$$\frac{dv_{Cr}}{dt} = \frac{1}{C_r} i_s \tag{10}$$

$$\frac{dv_R}{dt} = \frac{1}{C_p}\left(\frac{1}{n} i_s - i_R \right) \tag{11}$$

$$\frac{dV}{dt} = \frac{1}{C_f}\left(abs(i_R) - \frac{V}{R_{load}} \right) \tag{12}$$

where C_r, L_r, and R_r are the resonant tank's series capacitor, inductor and resistor, respectively. R_{load} is the load resistance; C_p is the resonant tank's parallel capacitor, and C_f is the output filter respectively.

The operation of the dc-dc resonant converter shows primarily sinusoidal waveforms for the ac sides and essentially

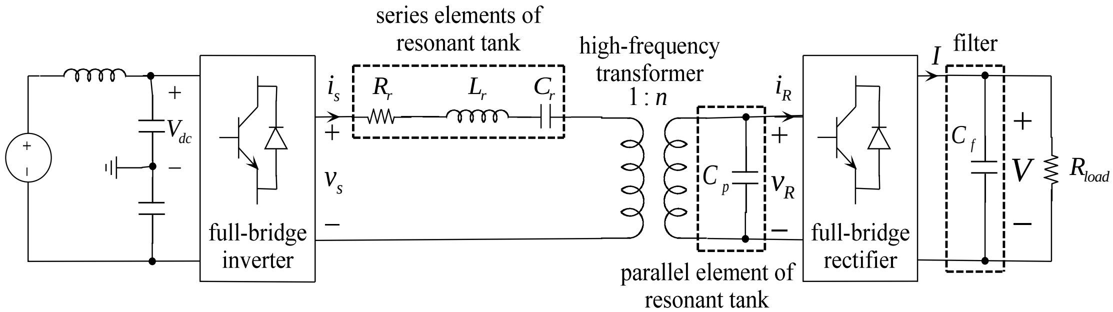

Fig. 2. Resonant circuit under consideration.

constant quantities on the dc sides. These are however overlaid by high-frequency switching components that have relatively small magnitudes. Therefore, in the development of an average-value model, only index zero (for dc) and index one (for ac) Fourier components are considered.

C. Average-Value Converter Model

The average model of the converter is obtained by applying the averaging operator to the converter equations given in equations (9) to (12). For dc variables the zero-order component ($k = 0$) is considered and for ac variable, the first-order component ($k = 1$) is considered.

IV. Model Validation and Simulation Results

In this section, the average-value model developed for the considered resonant converter is validated against a fully-detailed electromagnetic transient simulation model. The EMT model is developed in the PSCAD/EMTDC simulator and includes the high-frequency switching components of the response.

The multi-converter resonant circuit shown in Figure 3 is considered for this study. The circuit consists of 10 identical resonant converters each connecting a 250V dc source to a common dc bus. The identical resonant converters were used to simplify the modeling aspect of the test case and to demonstrate the computational complexity of the fully detailed EMT model. The simulation speed enhancement will remain unchanged even if different dc-dc converters were used. A dc-ac collector converter inverts the dc bus voltage to supply ac, fundamental-frequency power to an ac network. This converter system layout may occur, for example, when renewable energy sources or large-scale battery storage systems are to be pooled together and connected to an ac system. Table I shows specifications of the considered test case.

Average-value models of each converter are developed and interfaced to yield the average model of the entire converter system. An EMT model of the system is also developed. Identical test scenarios are followed for the two models for a simulation period of 4 seconds. Both models are run on an i7 processor at 2.80 GHz (8.00 GB RAM, 64-bit operating system).

TABLE I
Test System Specification

Quantity	Rating
Nominal dc bus voltage	980 V
Converter droop	1%
Rated power	50 kW
Rated voltage	1000 V

Table II compares the total simulation runtime of the detailed EMT model and the average-value model. As seen the simulation runtime has reduced drastically by using the average model. It should however be noted that with a larger number of converters the complexity of resulting system of equations will grow as well. Note that the reduced harmonic content of the average model allows use of a larger time step for representation of the limited harmonic components considered and hence contributes to the increase in the speed of simulation.

TABLE II
The Simulation Runtime Comparison

	Simulation time (s)	Time step
Detailed EMT model	3763	$2\,\mu s$
Average-value model	82	$50\,\mu s$

Figures 4 through 7 compare the detailed model and generalized state-space averaging model. The ac current and voltage waveforms on the HV side of the VSC are presented in Figures 4 and 5, respectively. DC bus current and voltage are shown in Figures 6 and 7, respectively. Except for the high-frequency switching content the generalized state-space averaging model demonstrates close conformity. Figure 8 shows the reference voltage waveforms generated by the detailed and the averaged models. Figure 9 presents the transient response of both models to a step change in the dc bus voltage.

Figures 10 through 13 compare the detailed model and generalized state-space averaging model during a dc fault on the positive rail of dc bus (see Figure 3). The average model follows a similar pattern during fault as the detailed model. There is however a small phase delay in the waveforms produced by the average model (only during the fault), which are attributed to the harmonic content of the controller input waveform during the fault.

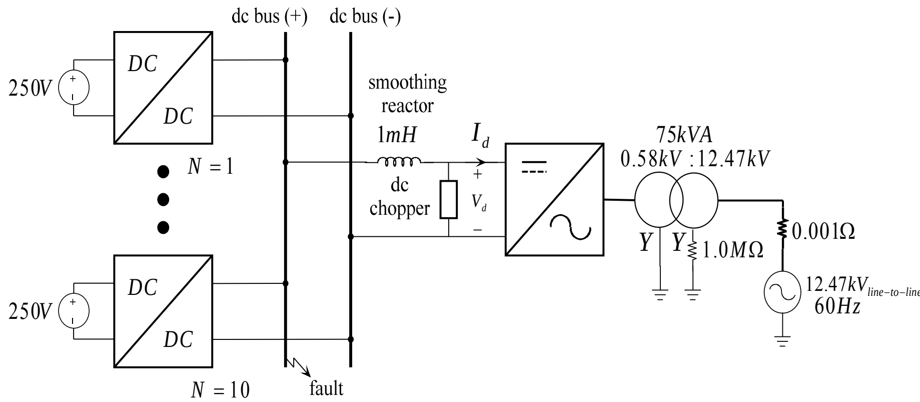

Fig. 3. A dc plant connected to a 60Hz grid through a VSC.

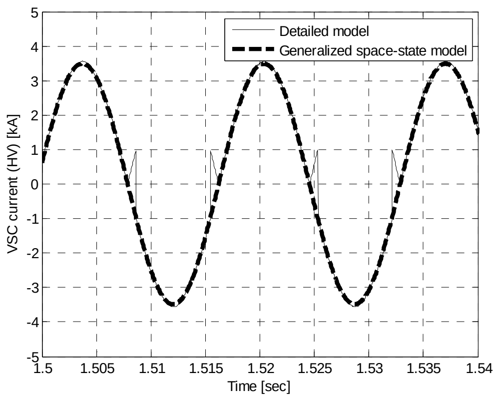

Fig. 4. Comparison of the VSC current (HV).

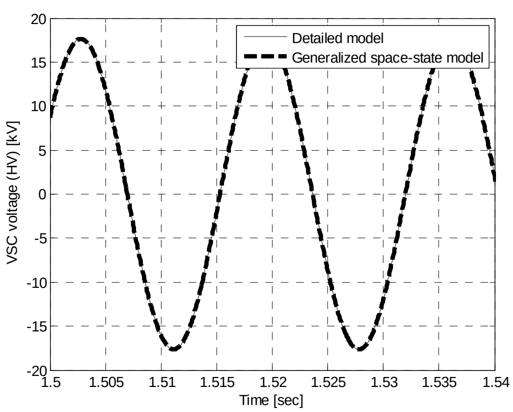

Fig. 5. Comparison of the VSC voltage (HV).

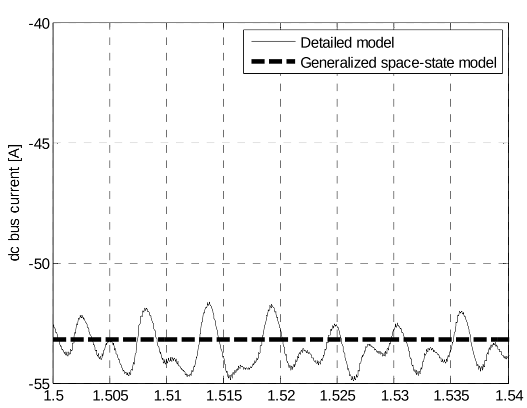

Fig. 6. Comparison of the dc bus current (I_d).

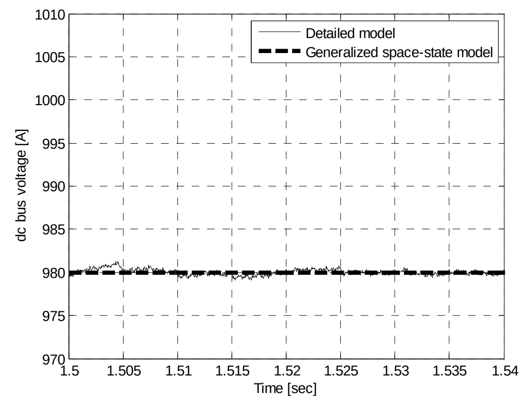

Fig. 7. Comparison of the dc bus voltage (V_d).

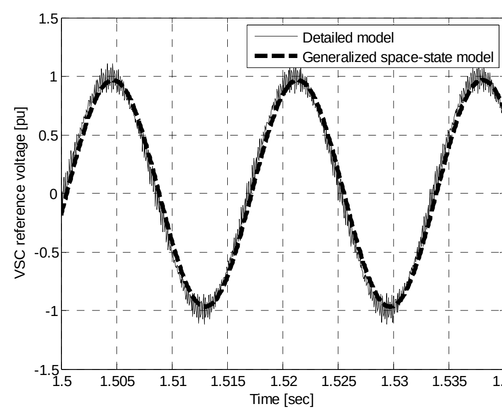

Fig. 8. Comparison of the VSC reference voltage.

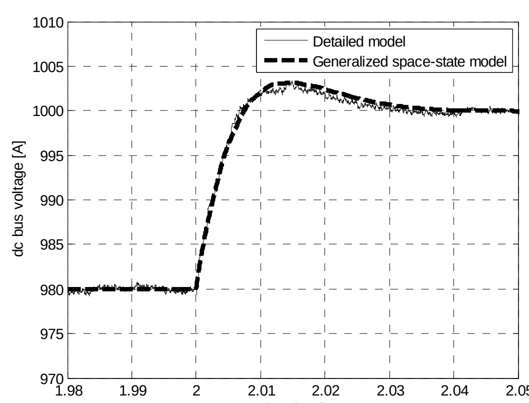

Fig. 9. Transient response comparison of dc bus voltage.

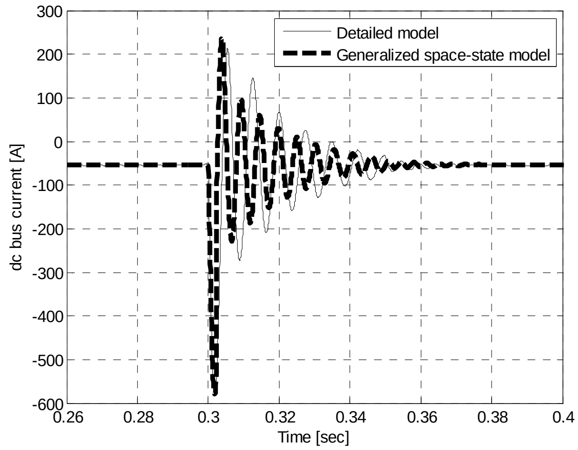

Fig. 10. Transient response comparison of dc bus current due to a dc fault.

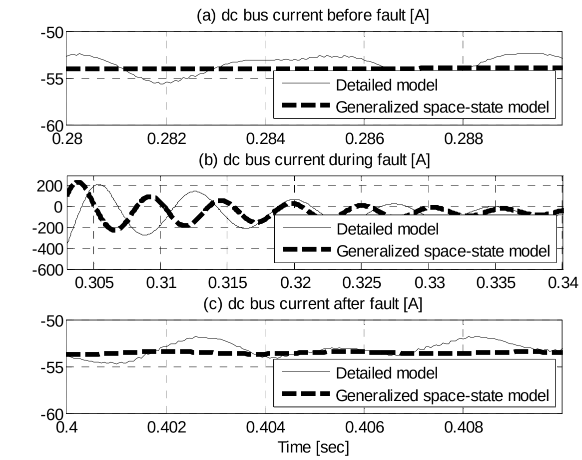

Fig. 11. DC bus current before, during and after a dc fault.

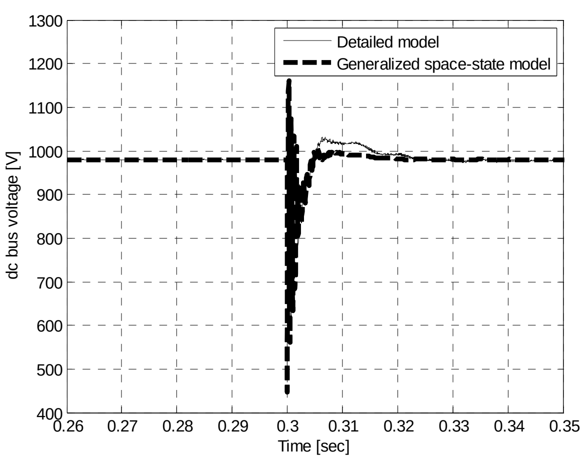

Fig. 12. Transient response of the dc bus voltage due to a dc fault.

V. Conclusions

The paper developed a generalized state-space averaging model to verify its computational efficiency in the simulation of high-frequency resonant converters. The average model was validated by comparing its response to the original circuit, in the simulation of a multi-converter dc-ac system. The results demonstrated the efficacy of the developed model in representing the average behavior of the system variables while reducing its simulation time step.

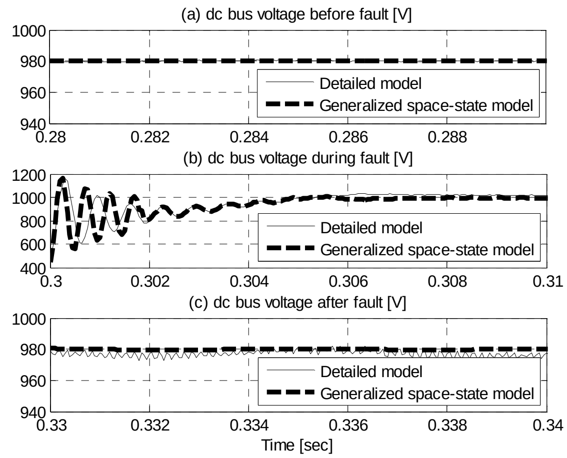

Fig. 13. DC bus voltage before, during and after a dc fault.

VI. References

[1] R.W. Erickson and D. Maksimović, *Fundamental of Power Electronics,* 2nd Ed. Norwall, MA: Kluwer Acdemic, 2001.

[2] Y. Zhang and P.C. Sen, "D-Q models for resonant converters," in *Power Electronics Specialists Conference,* Aachen, Germany, 2004, vol. 3, pp. 1749-1753.

[3] S. Golestan, M. Joorabian, H. Rastegar, A. Roshan and J.M. Guerrero, "Droop based control of parallel-connected single-phase inverters in D-Q rotating frame," in *Industrial Technology,* Churchill, Australia, 2009, pp. 1-6.

[4] F. Krismer, J. Biela and J.W. Kolar, "A comparative evaluation of isolated bi-directional dc/dc converters with wide input and output voltage range," in *Industry Application Conference*, Kowloon, Hong Kong, 2005, vol. 1, pp. 599-606.

[5] X. Li and A.K.S. Bhat, "Analysis and design of high-frequency isolated dual-bridge series resonant dc/dc converter," *IEEE Transactions on Power Electronics,* vol. 25, no. 4, pp. 850-862, 2010.

[6] H. Krishnaswai and N. Mohan, "Three-port series-resonant dc-dc converter to interface renewable energy sources with bidirectional load and energy storage ports," *IEEE Transactions on Power Electronics,* vol. 24, no. 10, pp. 2289-2297, 2009.

[7] S. Zheng and D. Czarkowski, "Dynamics of a phase-controlled series-parallel resonant converter," in *Circuits and Systems*, Scottsdale, Arizona, 2002, vol. 3, 819-822.

[8] S.R. Sanders, J.M. Noworolski, X.Z. Liu and G.C. Verghese, "Generalized averaging method for power conversion circuits," *IEEE Transactions on Power Electronics*, vol. 6, no. 2, pp. 251-259, 1991.

[9] J. Peralta, H. Saad, S. Dennetière, J. Mahseredjian and S. Nguefeu, "Detailed and averaged models for a 401-level MC-HVDC system," *IEEE Transactions on Power Delivery*, vol. 27, no. 3, pp. 1501-1508, 2012.

[10] A.Yazdani and R. Iravani, "A generalized state-space averaged model of the three-level NPC converter for systematic DC-voltage-balancer and current controller design," *IEEE Transaction on Power Delivery,* vol.20, no. 2, pp. 1105-1114, 2005.

[11] S.R. Rimmalapudi, S.S. Williamson, A. Nasiri and A. Emadi, "Validation of generalized state space averaging method for modeling and simulation of power electronic converters for renewable energy systems," *Journal of Electrical Engineering & Technology,* vol. 2, no. 2, pp. 231-240, 2007.

[12] A. Emadi, "Modeling and analysis of multiconverter DC power electronic system using the generalized state space averaging model," *IEEE Transactions on Industrial Electronics,* vol. 51, no. 3, pp. 661-668, 2004.